

AISC E&R Library ST910
7180

1056

→ research report file

subject: 1- Welding
2- Welded Connections

CONTINUED RESEARCH ON MECHANICAL PROPERTY IMPROVEMENTS IN ELECTROSLAG
WELDING OF HIGH STRENGTH, LOW ALLOY STEELS.

Final Report

Prepared for: American Institute of Steel Construction
400 N. Michigan Avenue
Chicago, IL 60611

Prepared by: MSNW, Inc.
P.O. Box 865
San Marcos, CA 92069

author
G. H. Reynolds, Principal Investigator

June 20, 1984

RR1056
7180

TABLE OF CONTENTS

SUMMARY	1
INTRODUCTION	3
REDUCED HEAT INPUT ELECTROSLAG WELDING EQUIPMENT	8
MATERIALS AND FILLER METALS	10
EVALUATION TECHNIQUES FOR WELDED TEST PLATES	13
WELDING PROCEDURE DEVELOPMENT AND TEST RESULTS	14
Solid Electrodes	14
Flux-Cored Electrodes	37
CONCLUSIONS	39
RECOMMENDATIONS	40

SUMMARY

This project was performed to examine a reduced heat input electroslag welding process using high alloy content filler metals for ASTM A588 steel. Reduced heat input was accomplished through the use of supplemental metal powder filler additions which permitted higher welding travel speeds, thereby reducing heat input to the base metal. Prior research has indicated that the combination of reduced heat input and high alloy filler metals could produce electroslag welds in ASTM A588 steel having greatly improved weldment mechanical properties, particularly impact strength, relative to conventional high heat input electroslag welds. Reduced heat input, high alloy powder addition electroslag welds were therefore prepared in A588 steel using both solid and flux-cored electrodes. Evaluation of the experimental weldments included weld metal chemical analysis, metallographic examination, transverse and all weld metal tensile tests, and detailed study of the impact strength at multiple locations across the weldments and over the temperature range -20° to $+32^{\circ}$ F.

Impact strength of both the solid and flux-cored electrode high alloy electroslag welds was consistently far superior to conventional electroslag welds for both weld metal and heat affected zone locations. For the weld metal, this was attributed to both finer weld metal grain sizes and higher weld metal alloy content, particularly nickel content. For the heat affected zone, this was attributed to reduced welding process heat input. Weld metal impact strength was as much as a factor of ten higher than usually observed for conventional electroslag welds while heat affected zone impact strengths were increased by as much as a factor of five. Solid electrode high alloy welds yielded superior properties to flux-cored electrode welds. Tensile properties of both the solid and flux-cored electrode welds easily met the requirements for welded A588 steel. The powder addition welding process was shown to be an effective method for refining both weld metal and heat affected zone microstructures. It was concluded that the process shows considerable promise for improving the reliability of electroslag welded structures of A588 steel and for reducing heavy section steel fabrication costs.

Recommendations were presented for development of a consumable guide tube version of the high alloy electrode/powder addition welding process which should be of wide applicability in structural steel fabrication. Additional recommendations were presented for detailed study of fatigue and fracture toughness properties of the improved electrosag weldments in A588 steel to further assess their suitability for industrial implementation by structural steel fabricators.

INTRODUCTION

Electroslag welding is an economical process for single-pass, vertical butt welding of heavy section steels. Weldments produced by the electroslag process exhibit a highly oriented, directionally solidified, columnar grain structure in the weld metal and a coarse-grained, recrystallized heat affected zone (HAZ). These features result from the method of heat removal via water-cooled shoes and the high heat input inherent in the electroslag process, respectively.

Numerous investigations have shown that the weld metal properties in electroslag weldments are both anisotropic and inhomogeneous. Weld metal mechanical properties are a cause for concern, particularly at the weld metal centerline where the columnar grains meet. This central zone of weld metal has been shown to possess inferior yield and tensile strength, ductility, and impact strength relative to other locations across the weldment and base metal. Also, the fatigue strength of the central zone is a frequent cause for concern. The inferior properties of the central zone are typically due to a combination of improper grain structure and insufficient alloy content.

Excessive grain growth is often observed within the base metal HAZ adjacent to the fusion line due to the exceptionally high heat input in electroslag welding. This excessive grain growth may lead to inferior properties within the HAZ, particularly for quenched and tempered steels. It is likely that significant properties can be realized only through post-weld heat treatment or through a fundamental modification to the conventional electroslag welding process which effects significant reductions in process heat input to the base metal.

The properties of both weld metal and HAZ may be equalized through normalizing which removes the highly oriented columnar-grained weld metal structure and the coarse-grained structure of the HAZ. Unfortunately this treatment is impractical for large structures such as bridge girders. Lower temperature heat treatments have been shown to effect some improvement in weldment properties but are also impractical for large structures. Techniques such as vibration of a consumable guide tube and welding electrode combined with alloy additions have recently

been shown to provide a measure of weld metal grain refinement, but since process heat input is not reduced, little, if any, improvement in HAZ properties can be expected. The most attractive method for improving weldment properties is one which incorporates significant improvements in the properties of single-pass welds in the as-welded condition, increases overall productivity, and is readily adapted to current industrial welding operations. Such a process, recently developed by MSNW, Inc., was originally demonstrated on A588 bridge steel under the sponsorship of the American Iron and Steel Institute (AISI) Steel Plate Producers Engineering Subcommittee.

The MSNW process is shown schematically in Figure 1. It is a narrow-gap process which utilizes supplemental filler metal in the form of metal powder, additional to that supplied by the consumable electrode, to increase the productivity of the welding operation while simultaneously decreasing process heat input. Metal powder is fed to the current-carrying electrode where it is held in place by the electromagnetic force field around the electrode and conveyed to the weld pool to be melted. The metal powder filler, when introduced into the weld pool, is melted by process heat which is normally wasted. The chilling effect of the metal powder on the weld pool reduces overheating of the weld metal and this produces grain refinement and other fundamental changes in the electroslag weld metal structure which may be used to advantage in improving weld metal properties. Since the contribution of the metal powder to the weld is in addition to that of the consumable welding electrode, total filler metal deposition rate is increased in direct proportion to the amount of metal powder added. The travel speed of the welding process is also increased in direct proportion to the amount of metal powder filler added. This results in a proportional decrease in process heat input to the base metal. Alloying additions needed for improved weld metal tensile or impact strength may be made through use of high alloy content electrodes or through the metal powder added to the process, or both.

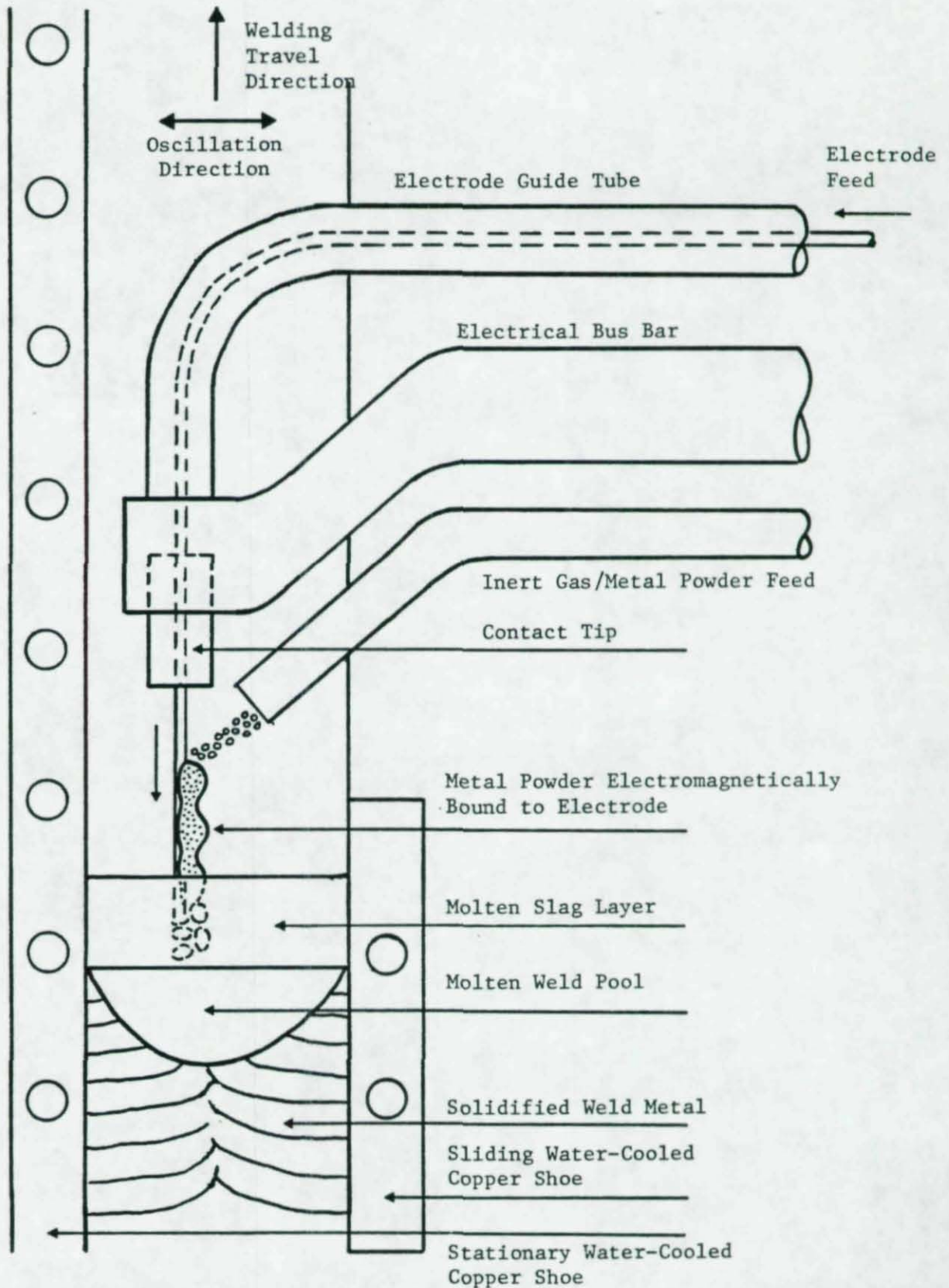


Figure 1. Schematic Cross Section of Reduced Heat Input, Metal Powder Addition Electroslag Welding Process

It has been shown in the original AISI-sponsored work on A588 that the reduced heat input of the MSNW electroslag process results in significantly smaller HAZ widths in the base metal and greatly reduced base metal penetration. Reduced base metal penetration is particularly important in electroslag welding of structural steels since it reduces the dominant influence of base metal contribution on final weld metal properties and allows the proper filler metal composition to be utilized to its fullest extent. The improved electroslag process with metal powder filler additions has produced as much as a 100% increase in total filler metal deposition rate accompanied by a 50% decrease in heat input to the base metal. Very encouraging results were demonstrated on A588 with both solid and flux-cored electrodes, including common flux-cored electrodes not normally used in electroslag welding. The improved process thus addresses the fundamental problems in electroslag welding of A588 by reducing process heat input to the base metal and providing a mechanism for improved control of weld metal composition.

The improved electroslag process utilizing metal powder filler additions is expected to provide the following benefits when fully developed and qualified for fabrication of A588 structural steel:

1. The greatly reduced heat input possible with the new technique results in significantly reduced base metal penetration during welding. Thus, the influence of base metal composition on weld metal properties is minimized and weld metal properties are more influenced by filler metal composition as desired.
2. The addition of alloying elements desired to meet weld metal property specifications may readily be made through addition of alloyed metal powder of the proper composition or use of highly alloy content electrodes, or both. For example, alloying additions through the metal powder or electrode may be made to increase weld metal tensile strength, impact strength, and presumably fatigue strength. This should be particularly useful in combination with the reduced base metal dilution contribution to the final weld metal composition.

3. The reduced heat input of the electroslog process with metal powder addition leads to reduced weld metal and HAZ thermal cycling. This in turn is expected to lead to improved weld metal and HAZ tensile, impact and fatigue properties through refinement of weld metal grain structure and reduction of the excessive grain growth commonly seen in the HAZ in conventional electroslog welding. The reduced weld metal and HAZ grain sizes are expected also to improve the inspectability of weldments by ultrasonic techniques.
4. The additional filler metal provided by the metal powder provides for greatly increased productivity of the electroslog welding process. On the basis of the results achieved to date on A588 and other steels, total metal deposition rates of approximately 70 lb/hr/electrode have been demonstrated for 3/32 in. diameter electrodes at metal powder/electrode weight ratios of approximately 1.0. It appears that total metal deposition rates on the order of 100 lb/hr/electrode are achievable in the welding of structural steels with common sized electrodes. This tremendous increase in process productivity and associated fabrication cost savings are accomplished in concert with improved weldment properties.
5. The metal powder provides additional filler metal of known chemistry and typically of much higher purity than the base metal. This means that the factors which lead to grain boundary separations, microfissuring, or hot cracking of electroslog welds are reduced in direct proportion to the amount of metal powder added.
6. The MSNW, Inc. process appears to be capable of improving the reliability and integrity of electroslog welds and restoring electroslog welding as a principal method for fabrication of heavy section structural steels.

In the preliminary AISI-sponsored research, a number of narrow-gap electroslog welds were prepared using solid (Linde WS) and flux-cored (Hobart Fabco 83) electrodes recommended for welding of A588 bridge steel. Experiments were performed with additions of varying amounts of metal powder to effect progressively larger reductions in welding process heat input. In addition, for a given ratio of metal powder to electrode, i.e., at a constant welding process heat input, various types of metal powder filler having different alloy contents and different oxygen contents were utilized. Both baseline and powder addition welds were prepared at much lower heat inputs than usually observed in

electroslag welding through the narrow-gap procedures used. Heat input has been reduced more than 50%. A limited number of experiments were performed with high alloy content solid electrodes.

Evaluation of these welds showed that weld metal tensile and impact properties were improved significantly through the reduced heat input metal powder addition electroslag welding process. Minimum heat affected zone impact properties were improved slightly by the reduced heat input process. Metallographic and chemical analysis of the welds showed that the expected benefits of reduced base metal penetration, reduced width of the heat affected zone, smaller weld metal and heat affected zone grain sizes, and improved control over weld metal composition, were realized. Particularly encouraging results were obtained with the high alloy content solid electrodes used in combination with high alloy content powder formulations. The present research was therefore undertaken to study the properties of high alloy content, reduced heat input, powder addition electroslag welds, produced with both solid and flux-cored electrodes, in greater detail. A number of experimental high alloy content welds were produced and subjected to extensive mechanical property testing and metallurgical evaluation.

REDUCED HEAT INPUT ELECTROSLAG WELDING EQUIPMENT

The equipment described here was constructed by MSNW, Inc. and used for preparation of reduced heat input electroslag welded test plates. The experimental welding apparatus is of the travelling-head type and was designed to perform either electroslag or electrogas welding using metal powder filler additions. Test plates up to 36.0 in. in length and 4.0 in. in width can be welded using a single, oscillated electrode. For welding of ferromagnetic filler metal compositions, the method used to introduce metal powder filler into an electroslag weld is to feed metal powder to the vicinity of the current-carrying electrode where it is held in place on the electrode by the electromagnetic field and conveyed into the metal/slag pool to be melted. An alternative way of making metal powder additions would be through the use of large diameter tubular electrodes with metal powder-containing cores. For simplicity, however, the MSNW, Inc. equipment utilizes loose metal powder metering and feeding. It has been found desirable to avoid the influence of stray magnetic fields on the loose powder and to use a flowing, inert shielding gas to assure that the metal powder is adequately conveyed to the electrode and does not bind in the dispensing apparatus.

The equipment was designed and constructed for test plate production with maximum flexibility in the adjustment of operating parameters. An overall view of the experimental apparatus is shown in Figure 2. The control console contains potentiometers for metal powder and flux metering systems, vertical travel speed, electrode feed rate and oscillation frequency. The apparatus uses a Linde 1000A constant potential power supply. A walk-around control box is provided which contains on-off controls for all necessary functions. The welding head assembly with wire reel, straightener, feeder (Lincoln LN-8), weld nozzle (Lincoln K-176) and crank type mechanical oscillator is shown in Figures 3 and 4. Figure 4 also shows the metering devices used to dispense metal powder or flux to the vicinity of the weld nozzle. Hoppers for metal powder and flux storage are located immediately above the metering devices. More detailed views of the metal powder and flux metering

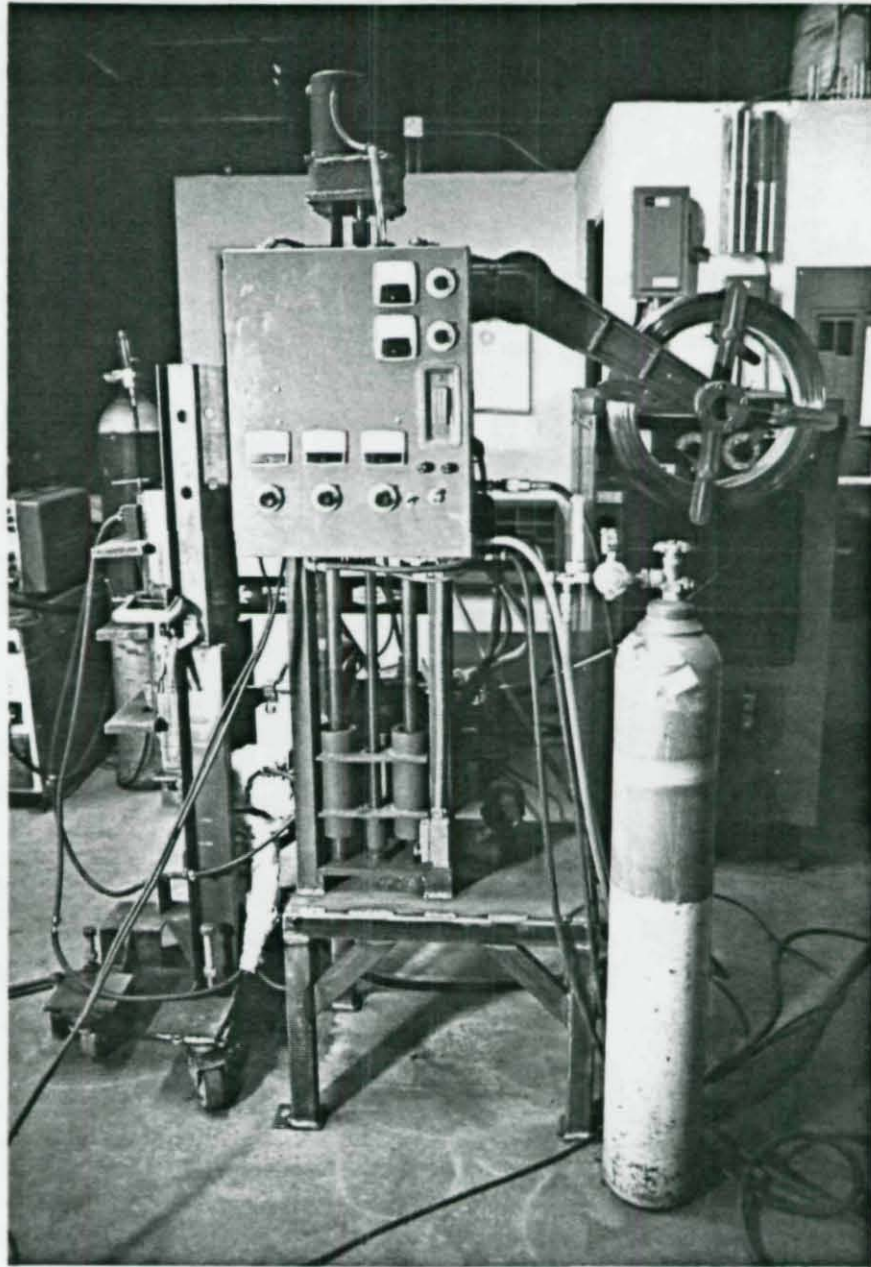


Figure 2. Overall View of Experimental Welding Apparatus, Control Panel and Power Supply.

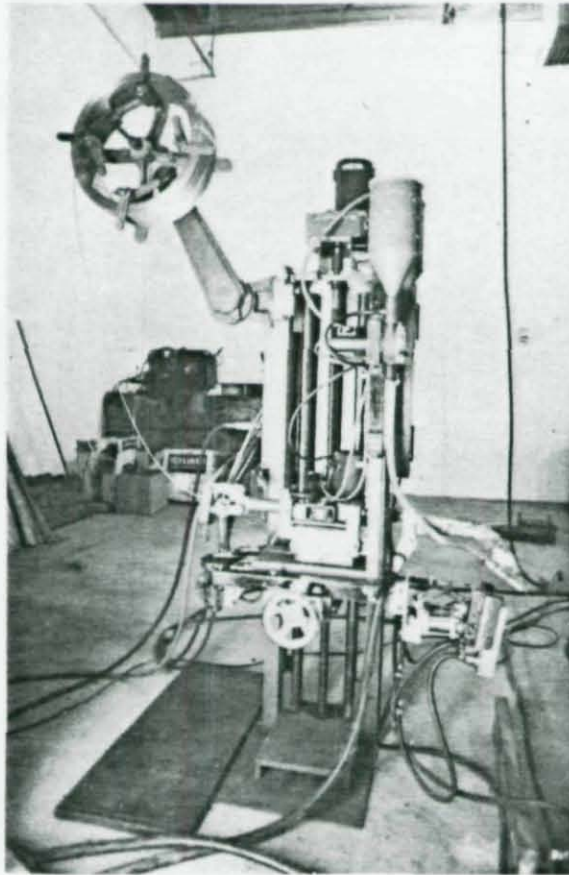


Figure 3. Weld Head Assembly, Overall View.

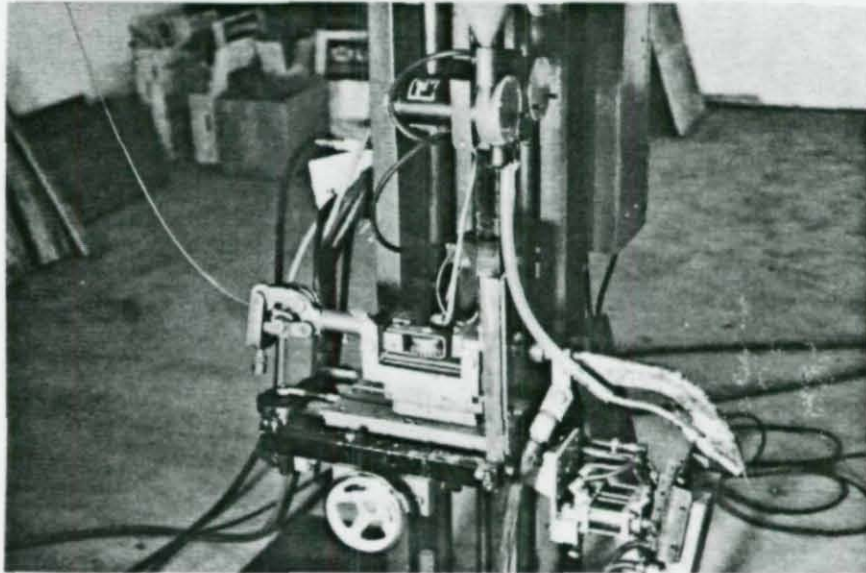


Figure 4. Weld Head Assembly, Detailed View of Wire Straightener, Wire Feed Rolls, Weld Nozzle, and Crank-Type Oscillator (Lower Left).

devices are shown in Figure 5. A shielding gas line for aiding in conveyance of the metal powder to the electrode via the plastic tube visible in Figure 4 is attached to the top of the metal powder metering device. A close-up of the weld nozzle, metal powder dispensing tube with replaceable ceramic cup, and the pneumatically activated water-cooled 6.0 in. copper shoe which travels with the welding head are shown in Figures 6 and 7. During welding, metal powder is fed to the vicinity of the welding electrode approximately 0.5 in. below the electrical contact tip. The powder is then held in place on the electrode by the magnetic field around the DC current-carrying electrode and carried into the molten slag pool to be melted in combination with the electrode. The entire welding head assembly is driven vertically by a variable-speed motorized ball screw.

The sliding and stationary water-cooled copper shoes used on the face and root sides of the weld, respectively, have a 0.0625 in. deep slot with a 90° included angle bevel and a 0.75 in. wide flat at the slot bottom to provide weld reinforcement. The cooling shoes are provided with a water interlock so that loss of water pressure during welding disengages the contactor in the power supply. Typical water flow rates during welding are 1.0 to 1.5 gpm. A test plate assembly fit-up and ready for welding is shown in Figure 8. Strongbacks and the stationary water-cooled copper shoe are clearly visible in this figure. Run-on tabs are normally used to begin welding. Run-off tabs are not normally used. An arc is struck at the bottom of the run-on section and flux is added until the arc is extinguished and the process is fully into the electroslog mode. When electroslog operation is achieved, metal powder additions are initiated. Steady-state electroslog operation is normally achieved after 1.0-2.0 in. of travel.

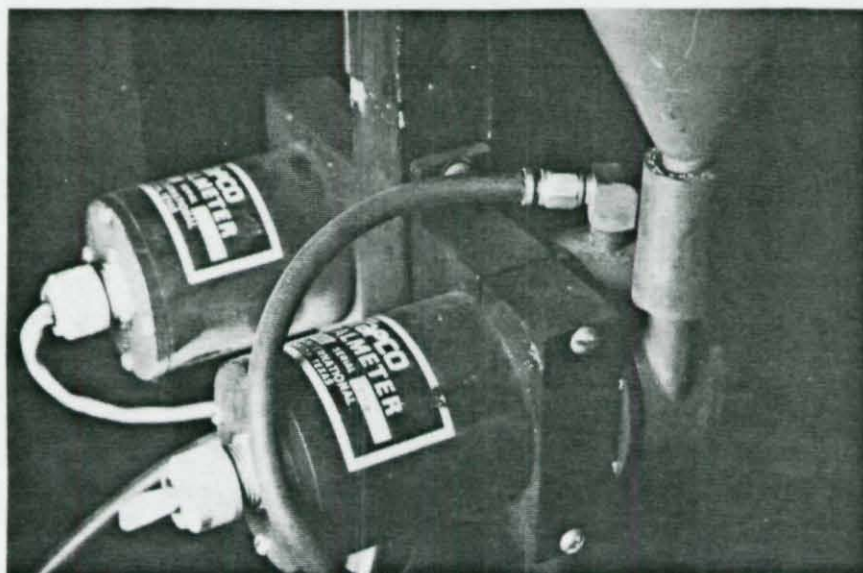


Figure 5. Metal Powder and Flux Metering Devices, Rear View. Note Shielding Gas Line to Metal Powder Metering Device.

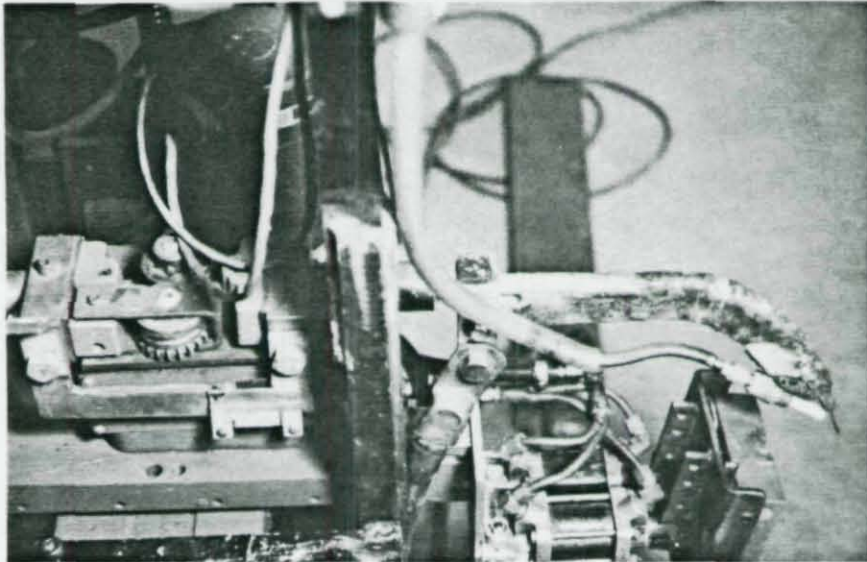


Figure 6. Weld Nozzle, Powder Dispensing Tube with Ceramic Cup and Pneumatically Controlled Sliding Water-Cooled Copper Shoe.

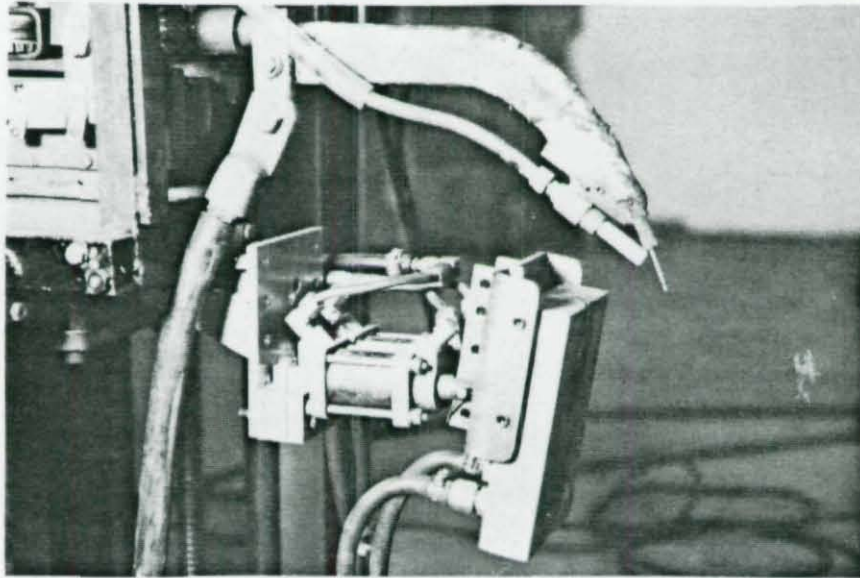


Figure 7. Same Components as Shown in Figure 6. Alternate View.

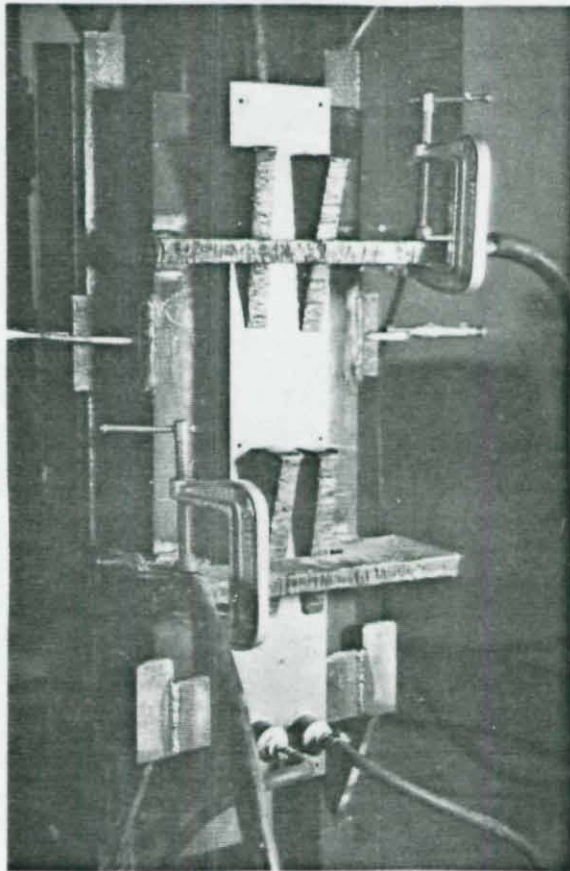


Figure 8. Test Plate Assembly Ready for Welding.

MATERIALS AND FILLER METALS

Mill certifications for the 2.0 in. thick ASTM A588, Grade H plate used for production of experimental weldments are shown in an Appendix to this report. Test plates were cut with a mechanized oxyacetylene cutting apparatus. Flame cut surfaces on which welding would be performed were ground to remove scale prior to welding. The length of each experimental weld was 18.0 inches.

Three solid, high alloy electrodes were used to prepare experimental weldments. These were Airco AX-90, Linde 95, and Linde 44. The nominal composition of each is shown in Table 1. Airco AX-90 and Linde 95 are both high Ni content electrodes while Linde 44 is a high Mn, lower Ni content composition. Diameter for all solid electrodes was 0.093 inch. Two flux-cored, high alloy electrodes were used. These were Hobart Fabco 805 and Linde FC-727. The nominal deposited composition of the Linde FC-727 electrode is shown in Table 1. The Hobart Fabco 805 electrode is presently developmental and the exact deposited composition is proprietary data, however, the composition is similar to that of the Linde FC-727 electrode. Diameter for both flux-cored electrode was 0.062 inch.

Two blended metal powder formulations were prepared for use with the solid electrodes. The compositions of these two formulations are shown in Table 1. Type AX-90 powder was used with both the AX-90 and Linde 95 electrode. The Type 44 powder has a significantly higher Ni content than the Linde 44 electrode. One blended metal powder formulation, designated FC-727 and shown also in Table 1, was used with both the Hobart Fabco 805 and Linde FC-727 flux-cored electrodes. The powder composition differs significantly from the deposited electrode compositions only in Mo content.

Table 1

NOMINAL COMPOSITIONS (Wt.%) OF FILLER METALS USED

<u>Element</u>	<u>Airco AX-90</u>	<u>Linde 95</u>	<u>Electrodes</u>		
			<u>Linde 44</u>	<u>Hobart Fabco 805</u>	<u>Linde FC-727</u>
C	0.08	0.06	0.13	*	0.05
Mn	1.27	1.65	2.05	*	0.80
Si	0.38	0.35	0.12max	*	0.30
Mo	0.43	0.35	0.45	*	----
Ni	1.90	1.75	0.65	*	2.20
Cr	0.06	0.10	----	*	----

* Composition proprietary to Hobart Brothers Company

Table 1 (continued)

NOMINAL COMPOSITIONS (Wt.%) OF FILLER METALS USED

<u>Element</u>	<u>Powders</u>		
	<u>AX-90</u>	<u>44</u>	<u>FC 727</u>
C	0.04	0.05	0.03
Mn	1.27	2.05	0.80
Si	0.40	0.20	0.30
Mo	0.49	0.49	0.45
Ni	1.90	1.80	2.20
Cr	----	----	----

01636

EVALUATION TECHNIQUES FOR WELDED TEST PLATES

Welded test plates were evaluated in the as-welded condition. Chemical analysis of the weld metal was performed at the weld metal centerline, midthickness (i.e. center/center) location. Metallographic sections were polished and etched in H_2O -10% HNO_3 . Heat affected zone widths were measured on each side of the weld at the midthickness of the plate and averaged. Selected welds were polished and etched with 2% Nital and used for microexamination including quantitative grain size determination.

Two subsized tensile specimens were prepared from each experimental weldment. Longitudinally oriented specimens consisted entirely of weld metal and the specimen axis was parallel to the direction of welding. Transverse specimens had a gage length consisting entirely of weld metal but the specimen axis was perpendicular to the direction of welding. The two orientations tested provide information on the directionality of weld metal mechanical properties. Fully instrumented tensile tests were performed.

Charpy V-notch impact tests were performed on each plate for weld metal and heat affected zone locations. Base metal impact tests were performed on two plates and averaged. For preliminary screening, each experimental weldment was impact tested at $0^\circ F$ with specimen notch locations at the weld metal centerline (center/center) and in the heat affected zone 2.0mm from the fusion line. Direction of crack propagation was parallel to the direction of welding, and in an isostructural plane. These notch locations are usually observed to be the minimum impact strength locations and had been observed to be such in our prior work on A588 electroslag welds. Following screening impact tests, selected welds were used for additional CVN impact tests with the notch locations at the weld metal centerline, weld metal quarter width (i.e. in the middle of the columnar grained region), fusion line, fusion line plus 2.0mm, and fusion line plus 4.0mm. Testing was performed at $+32$, 0 , and $-20^\circ F$ to provide an indication of impact strength transition temperatures.

WELDING PROCEDURE DEVELOPMENT AND TEST RESULTSSolid Electrodes

Six experimental welds were prepared in the 2.0 in. thick A588 plate using solid, high alloy content electrodes. Five of these were prepared with metal powder additions while one was prepared with no metal powder additions for comparison purposes. All powder addition welds used a powder/electrode weight ratio of 0.75.

Table 2 shows the welding process parameters used to prepare each of the six experimental welds. (Additional welds were prepared while procedures were being developed, however the six shown represent preliminary optimum welding parameters and were suitable for testing.) Welding process parameters were held essentially constant for each of these welds, however joint configuration was varied slightly resulting in a variation in vertical travel speed which determines base metal heat input if voltage and current are held constant.

Experimental test welds 3A and 5A were prepared using the AX-90 electrode and AX-90 powder with square butt and single bevel joint designs of differing cross sectional area resulting in differing heat inputs. Test weld 13A was prepared using the Linde 44 electrode and Type 44 powder combination. Test weld 15A was prepared using the Linde 95 electrode with no metal powder addition. Even though the electrode feed rate is identical to that used for the analogous powder addition welds 7A and 9A, it is noteworthy that the welding current for 15A is significantly lower than for the powder addition welds. This is due to the fact that with no metal powder present the electrical resistivity of the molten slag is raised significantly. This leads to more I^2R heating in the current-carrying slag and a consequent decrease in the welding current required to melt the electrode for a constant electrode feed rate. The heat input for weld 15A is therefore approximately 20-25% higher than for the powder addition welds of similar joint cross-sectional area due primarily to the lower vertical travel speed rate used.

Table 2

WELDING PARAMETERS - 2.0 in. THICK ASTM A588 PLATE

Electrode Type	Airco AX-90	Airco AX-90	Linde 95
Electrode Diameter (in.)	0.093	0.093	0.093
Flux Type	Linde 124	Linde 124	Linde 124
Metal Powder Type	AX-90	AX-90	AX-90
Joint Design			
Type	Square Butt	Single Bevel	Single Bevel
Included Angle(°)	0	10	10
Root Opening (in.)	0.75	0.75	0.75
Electrode Oscillation			
Distance (in.)	1.125	1.125	1.31
Preheat (°F)	None	None	None
Shielding Gas/Flow Rate (cfm.)	Ar/15	Ar/15	Ar/15
Water Flow Rate (gpm.)	1.2	1.2	1.2
Voltage (V,DCRP)	38	38	38
Amperage (A)	460	460	460
Travel Speed (ipm.)	2.02	1.81	1.75
Metal Powder/Electrode Weight Ratio	0.75	0.75	0.75
Total Metal Deposition Rate (lbs./hr.)	49.6	49.6	49.6
Heat Input (J/in.)	519,200	579,400	599,300
Weld Identification Number	3A	5A	7A

Table 2 (continued)

WELDING PARAMETERS - 2.0 in. THICK ASTM A588 PLATE

Electrode Type	Linde 95	Linde 44	Linde 95
Electrode Diameter (in.)	0.093	0.093	0.093
Flux Type	Linde 124	Linde 124	Linde 124
Metal Powder Type	AX-90	44	None
Joint Design			
Type	Single Bevel	Single Bevel	Single Bevel
Included Angle (°)	10	10	10
Root Opening (in.)	0.625	0.625	0.625
Electrode Oscillation Distance (in.)	1.31	1.31	1.31
Preheat (°F)	None	None	None
Shielding Gas/Flow Rate (cfm.)	Ar/15	Ar/15	Ar/20
Water Flow Rate (gpm.)	1.2	1.0	1.3
Voltage (V,DCRP)	38	38	38
Amperage (A)	460	380	330
Travel Speed (ipm.)	1.94	1.874	1.125
Metal Powder/Electrode Weight Ratio	0.75	0.75	0.0
Total Metal Deposition Rate (lbs./hr.)	49.6	49.6	28.4
Heat Input (J/in.)	540,600	462,100	668,800
Weld Identification Number	9A	13A	15A

Table 2 (continued)

WELDING PARAMETERS - 2.0 in. THICK ASTM A588 PLATE

Electrode Type	Hobart Fabco 805	Linde FC-727
Electrode Diameter (in.)	0.062	0.062
Flux Type	Linde 124	Linde 124
Metal Powder Type	FC 727	FC 727
Joint Design		
Type	Single Bevel	Single Bevel
Included Angle (°)	10	10
Root Opening (in.)	0.625	0.625
Electrode Oscillation Distance (in.)	1.500	1.500
Preheat (°F)	None	None
Shielding Gas/Flow Rate (cfm.)	Ar/15	Ar/15
Water Flow Rate (gpm.)	1.3	1.3
Voltage (V, DCRP)	39	38
Amperage (A)	320	330
Travel Speed (ipm.)	1.15	1.07
Metal Powder/Electrode Weight Ratio	0.6	0.6
Total Metal Deposition Rate (lbs/hr.)	23.8	23.8
Heat Input (J/in.)	651,100	703,200
Weld Identification Number	17A	21A

Several comparisons are possible using these experimental weldments. Comparison of the results of evaluations of welds 7A and 9A versus 15A shows the effect of powder additions (i.e. lower heat input) on weldment properties. Comparison of welds 13A versus 5A, 7A, or 9A provides information on the gross effects of total weld metal alloy content since 13A has a significantly lower alloy content. Comparison of 5A versus 7A provides information on the effects of minor variations in weld metal alloy content at equivalent heat inputs.

As described previously, test plates 3A and 5A were prepared using the AX-90 electrode and matching composition AX-90 blended powder. Due to a slight difference in joint cross section geometry, plate 3A was prepared with 10% lower welding process heat input than plate 5A (519 vs. 570 KJ/in.). Weld metal chemical analyses for plates 3A and 5A are shown in Table 3. Chemical analyses were performed at centerline/midthickness of the weld. The analyses are consistent with the electrode and metal powder compositions used and with relatively low dilution of the weld metal by the base plate. Test plates 7A and 9A were prepared using the Linde 95 electrode with a slightly undermatching AX-90 powder. Again, variations in joint geometry account for a 10% difference in process heat input for these two plates (599 and 541 KJ/in. for 7A and 9A, respectively). Weld metal chemical analyses for plates 7A and 9A are shown in Table 3. The analyses agree well with each other and are consistent with the higher Mn content and lower Ni content of the Linde 95 electrode relative to the AX-90 electrode used to prepare plates 3A and 5A. Test plate 13A was prepared with the Linde 44 electrode/Type 44 powder combination at a heat input of 462 KJ/in. The weld metal chemical analysis shown in Table 3 is consistent with the lower Ni content (0.98 wt.%) and higher Mn content (1.49 wt.%) of this filler metal compared to AX-90 and Linde 95. Test plate 15A was prepared with the Linde 95 electrode and no metal powder additions. Weld metal composition shown in Table 3 is lower in Ni and Mo and higher in C than the analogous powder addition welds 7A and 9A because of greater dilution of the weld by the base metal caused by higher heat input for weld 15A. In general, the weld metal compositions observed agree well with the filler metal types and welding process parameters used.

Table 3

WELD METAL CHEMICAL ANALYSIS (Wt.%) at WELD CENTERLINE
A 588 Grade H Plate

<u>Element</u>	<u>I.D. No.</u>			
	<u>3A</u>	<u>5A</u>	<u>7A</u>	<u>9A</u>
C	.05	.06	.04	.04
Mn	1.05	.96	1.18	1.15
Si	.36	.27	.27	.27
P	.011	.009	.010	.011
S	.013	.012	.011	.012
Cr	.09	.31	.09	.10
Ni	1.66	1.96	1.63	1.52
Mo	.39	.45	.37	.34
O ₂	.055	.046	.043	.054
Fe	Balance	Balance	Balance	Balance

Table 3 (continued)

WELD METAL CHEMICAL ANALYSIS. (Wt.%) at WELD CENTERLINE
A 588 Grade H Plate

<u>Element</u>	<u>I.D. No.</u>			
	<u>13A</u>	<u>15A</u>	<u>17A</u>	<u>21A</u>
C	0.08	0.07	0.04	0.02
Mn	1.49	1.19	0.77	0.75
Si	0.10	0.39	0.32	0.34
P	0.015	0.011	0.010	0.013
S	0.015	0.011	0.015	0.016
Cr	0.08	0.12	0.04	0.07
Ni	0.98	1.23	2.04	1.89
Mo	0.35	0.20	0.20	0.18
Cu	0.16	0.13	0.07	0.10
O ₂	0.031	0.038	0.035	0.033
Fe	Balance	Balance	Balance	Balance

Both longitudinal and transverse all weld metal instrumented tensile tests were performed on each of the six test plates. Subsize tensile specimens were used having a 0.25 in. diameter gage section. Transverse specimens used a subsize gage length of 0.50 in. as well to assure that weld metal properties were being measured directly. Table 4 shows the results of the weld metal tensile tests for each plate. All welds show similar levels of yield and tensile strength, elongation, and reduction in area and easily meet the requirements (55 Ksi YS) for A588. For each weld, because of the very strong preferred orientation of columnar grains in the electroslag weld metal, transverse tensile strengths and percent elongation are lower than in the welding travel (longitudinal) direction while transverse percent reduction in area is higher. Transverse yield strength is lower than longitudinal yield strength, except for welds 5A and 15A. It is interesting to note that weld 13A prepared with lower alloy content Linde 44 and Type 44 filler metals shows the highest longitudinal yield and tensile strengths observed. There do not appear to be significant differences in tensile properties among the other experimental welds.

Screening Charpy V-notch impact tests were performed on specimens from weld metal, heat affected zone, and base metal locations. Weld metal specimens were taken at the weld metal centerline/midthickness (i.e. center/center) location since this is typically the location of minimum weld metal impact strength. Heat affected zone specimens were prepared with the notch location 2.0mm from the fusion line since, in our prior work on electroslag welding of A588, this was found to be the minimum impact strength location in the heat affected zone. Preliminary impact tests were performed at 0°F. The results for all six test plates are shown in Table 5. All results are reported and there were no discards or retests of low values. Base metal results shown in Table 5, well removed from the location of the weld, are 12.0 ft-lbs. average but range from 6 to 24 ft-lbs. Test plates 3A and 5A, prepared with the AX-90 electrode, show significantly different average impact strengths for the weld metal but similar values for the heat affected zone. Plate 5A, prepared at the higher heat input, shows the higher weld metal impact strength, 69.5 vs. 35.0 ft-lbs. Higher nickel and lower oxygen

Table 4

TENSILE TEST RESULTS

A 588 Grade H Plate

As-Welded Condition

<u>I.D. No.</u>	<u>Orientation</u>	<u>YS(Ksi)</u>	<u>UTS(Ksi)</u>	<u>% Elongation</u>	<u>% R.A.</u>
3A	Long.	71.1	92.1	27	61
	Transv.	57.4	77.2	16	74
5A	Long.	68.8	90.6	26	62
	Transv.	68.6	87.4	16	66
7A	Long.	68.6	90.6	29	68
	Transv.	60.8	81.0	17	71
9A	Long.	69.2	89.2	26	64
	Transv.	62.3	77.5	16	72
13A	Long.	71.6	97.4	23	65
	Transv.	62.6	74.0	21	75
15A	Long.	65.1	88.7	29	68
	Transv.	65.2	74.9	21	71
17A	Long.	64.7	85.9	20	43
	Transv.	58.1	74.2	21	68
21A	Long.	65.3	85.0	19	59
	Transv.	63.3	85.9	20	51

Table 5

CHARPY V-NOTCH IMPACT TEST RESULTS

A 588 Grade H Plate. As-Welded Condition.

Test Temperature 0°F

<u>I.D. No.</u>	<u>Location</u>	<u>Impact Strength (Ft-lbs.)</u>
3A	WM*	34.5
		38.5
		32.0
		Avg. 35.0
3A	HAZ**	23.0
		12.0
		12.0
		Avg. 15.7
5A	WM	77.5
		60.5
		70.5
		Avg. 69.5
5A	HAZ	10.0
		9.5
		25.0
		Avg. 14.9
7A	WM	84.0
		58.0
		56.0
		Avg. 66.0
7A	HAZ	49.0
		48.0
		44.5
		Avg. 47.2

*Weld Metal Centerline, Midthickness of Plate

**Heat Affected Zone, Notch Location 2.0 mm from Fusion Line,
Midthickness of Plate

Table 5 (continued)

<u>I.D. No.</u>	<u>Location</u>	<u>Impact Strength (Ft-lbs.)</u>
9A	WM	55.0 53.0 71.0 Avg. 59.9
9A	HAZ	29.5 56.0 53.5 Avg. 46.4
13A	WM	40.0 35.0 42.5 Avg. 39.2
13A	HAZ	48.5 28.0 14.5 Avg. 30.4
15A	WM	17.5 19.0 17.0 Avg. 17.9
15A	HAZ	31.0 7.5 8.0 Avg. 15.5
17A	WM	30.5 19.0 21.5 Avg. 23.7
17A	HAZ	17.5 15.0 12.0 Avg. 14.9

Table 5 (continued)

<u>I.D. No.</u>	<u>Location</u>	<u>Impact Strength (Ft-lbs.)</u>
21A	WM	8.5
		16.0
		10.5
		Avg. 11.7
21A	HAZ	9.0
		10.5
		30.0
		Avg. 16.5
Base Metal		11.5
		8.0
		9.5
		7.0
		9.5
		10.5
		6.0
		24.0
		22.5
Avg. 12.0		

content in the weld metal (Table 3) might account for some of the differences in weld metal impact strength between plates 3A and 5A. Test plates 7A and 9A, prepared with the Linde 95 electrode, show consistently high weld metal impact strength, 66.0 and 59.9 ft.-lb., respectively. These two welds also show much higher levels of heat affected zone impact strength 47.2 and 46.4 ft-lbs., than exhibited by plates 3A and 5A which averaged approximately 15 ft-lbs. The origin of these differences in heat affected zone impact strength are unclear since the overall process heat input is similar for all four test plates. It is very important to note here that the impact strengths measured on all four welds are far higher than would be observed in a conventional electroslag weld in A588 (ca. 3-6 ft/lbs. at the weld metal centerline). Thus our objective of demonstrating significantly improved as-welded mechanical properties in high alloy, powder addition welds has been satisfied.

Test plate 13A, prepared with the lower alloy content Linde 44/Type 44 filler metals shows lower weld metal impact strength than welds 5A, 7A, and 9A but higher impact strength than weld 3A. Heat affected zone impact strength is higher than welds 3A and 5A but lower than welds 7A and 9A. Since weld 13A was the lowest overall heat input weld it would have been expected to show the highest heat affected zone impact strength which was not the case. Test plate 15A, prepared with the Linde 95 electrode and no powder additions, shows significantly lower weld metal and heat affected zone impact strength than its powder addition analogs, 7A and 9A. Since this was the highest overall heat input weld, it would be expected to show the lowest weld metal impact strength of the high alloy welds and the lowest overall heat affected zone impact strength. This seems to be at least partly the case with respect to weld metal impact strength. Welds 3A and 5A show similar low heat affected zone impact strength to weld 15A, however.

Additional CVN impact tests were performed on welds 7A, 9A, and 13A at a variety of temperatures and locations since these three welds exhibited the best heat affected zone properties in the 0°F screening tests. Welds 7A and 9A also exhibited high weld metal impact strengths at 0°F. The results of the additional tests are shown in Table 6. Data from Table 5

Table 6

CHARPY V-NOTCH IMPACT TEST RESULTS

<u>I.D. No.</u>	<u>Location</u>	<u>Test Temperature (°F)</u>	<u>Impact Strength (Ft-lbs.)</u>
7A	WMC*	+32	63.5
			74.0
			Avg. 68.8
7A	WMC	0	84.0
			58.0
			Avg. 66.0
7A	WMC	-20	36.5
			49.0
			Avg. 42.8
7A	WMQ**	0	81.5
			88.0
			Avg. 84.8
7A	FL***	+32	51.0
			48.5
			Avg. 49.8
7A	FL	0	54.5
			14.5
			Avg. 34.5
7A	FL	-20	26.0
			18.5
			Avg. 22.3

* WMC = Weld Metal Centerline

** WMQ = Weld Metal Quarter Width

*** FL = Fusion Line

Table 6 (continued)

CHARPY V-NOTCH IMPACT TEST RESULTS

<u>I.D. No.</u>	<u>Location</u>	<u>Test Temperature (°F)</u>	<u>Impact Strength (Ft-lbs.)</u>
7A	FL + 2mm	+32	24.5
			60.0
			Avg. 42.3
7A	FL + 2mm	0	49.0
			48.0
			44.5
			Avg. 47.2
7A	FL + 2mm	-20	42.0
			35.0
			Avg. 38.5
7A	FL + 4mm	+32	70.5
			59.5
			Avg. 65.0
7A	FL + 4mm	0	25.5
			55.0
			Avg. 40.3
7A	FL + 4mm	-20	20.5
			23.0
			Avg. 21.8

Table 6 (continued)

CHARPY V-NOTCH IMPACT TEST RESULTS

<u>I.D. No.</u>	<u>Location</u>	<u>Test Temperature (°F)</u>	<u>Impact Strength (Ft-lbs.)</u>
9A	WMC	+32	95.5
			76.5
			Avg. 86.0
9A	WMC	0	55.0
			53.0
			Avg. 59.9
9A	WMC	-20	52.5
			78.5
			Avg. 65.5
9A	WMQ	0	83.0
			80.0
			Avg. 81.5
9A	FL	+32	46.0
			42.0
			Avg. 44.0
9A	FL	0	17.0
			49.0
			Avg. 33.0
9A	FL	-20	9.0
			40.5
			Avg. 24.8
9A	FL + 2mm	+32	81.5
			73.5
			Avg. 77.5

Table 6 (continued)

CHARPY V-NOTCH IMPACT TEST RESULTS

<u>I.D. No.</u>	<u>Location</u>	<u>Test Temperature (°F)</u>	<u>Impact Strength (Ft-lbs.)</u>
9A	FL + 2mm	0	29.5
			56.0
			53.5
			Avg. 46.4
9A	FL + 2mm	-20	7.0
			42.5
			Avg. 24.8
9A	FL + 4mm	+32	96.5
			90.5
			Avg. 93.5
9A	FL + 4mm	0	64.5
			84.0
			Avg. 74.3
9A	FL + 4mm	-20	37.5
			38.5
			Avg. 38.0

Table 6 (continued)

CHARPY V-NOTCH IMPACT TEST RESULTS

<u>I.D. No.</u>	<u>Location</u>	<u>Test Temperature (°F)</u>	<u>Impact Strength (Ft-lbs.)</u>
13A	WMC	+32	58.5
			65.0
			Avg. 61.8
13A	WMC	0	40.0
			35.0
			Avg. 39.2
13A	WMC	-20	42.0
			30.0
			Avg. 36.0
13A	WMQ	0	75.0
			76.0
			Avg. 75.5
13A	FL	+32	12.5
			9.0
			Avg. 10.8
13A	FL	0	10.5
			8.0
			Avg. 9.3
13A	FL	-20	5.5
			7.0
			Avg. 6.3
13A	FL + 2mm	+32	50.0
			87.0
			Avg. 68.5

Table 6 (continued)

CHARPY V-NOTCH IMPACT TEST RESULTS

<u>I.D. No.</u>	<u>Location</u>	<u>Test Temperature (°F)</u>	<u>Impact Strength (Ft-lbs.)</u>
13A	FL + 2mm	0	48.5
			28.0
			14.5
			Avg. 30.4
13A	FL + 2mm	-20	5.0
			41.0
			Avg. 23.0
13A	FL + 4mm	+32	28.0
			48.5
			Avg. 38.3
13A	FL + 4mm	0	53.5
			56.0
			Avg. 54.8
13A	FL + 4mm	-20	44.0
			20.0
			Avg. 32.0

is also reshowed in Table 6 for comparison purposes. Table 6 requires careful study since it contains much of interest. Comparing the weld metal centerline impact strength data over this temperature range for all three welds, the higher alloy content welds show higher impact transition temperatures than the lower alloy content weld (13A). Weld metal properties for all three welds are extremely encouraging. At 0°F, each weld shows that at the weld metal quarter width location (in the middle of the columnar zone), impact strength is significantly higher than for the weld metal centerline location and is not significantly affected by alloy content. The origin of this effect probably lies with the segregation of alloying elements or impurities to grain boundaries. When such grain boundaries are in the fracture plane as at the weld metal centerline, fracture resistance is lowered for the low alloy content weld (13A). At the quarter width location, most, if not all, grain boundaries are perpendicular to the fracture plane and their effect is eliminated.

For welds 7A and 9A, the heat affected zone impact strengths at the fusion line and fusion line plus 2.0mm locations are similar. For weld 13A however, fusion line impact strength is much lower than at the fusion line plus 2.0mm location. For all three welds, the fusion line plus 4.0mm location shows much higher impact strength than the other two heat affected zone locations. Weld 13A, which shows the lowest heat affected zone impact strength at the fusion line is both the lowest alloy content and lowest heat input weld. The origin of the exceptionally low fusion line impact strength is unclear. In general, however, the observed heat affected zone impact strengths over the observed temperature range must be considered extremely encouraging for the reduced heat input electroslag welding process using high alloy content filler metals.

Metallographic specimens were prepared from each welded test plate. Specimens were polished and etched in H₂O-10% HNO₃. Heat affected zone widths were measured on both sides of the weld at the midthickness of the plate and averaged. Figures 9 and 10 show the weldment microstructures observed for test plates 3A and 5A while heat affected zone widths are shown in Table 7. Lack of fusion (slag entrapment) defects are present

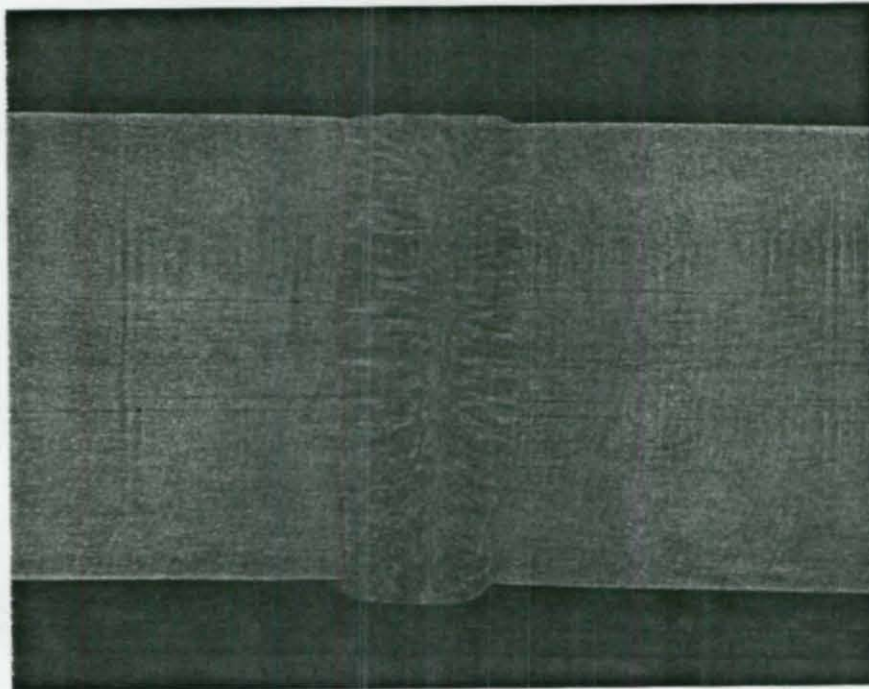


Figure 9. Metallographic Section, Welded Test Plate No. 3A. Magnification 1.2 x.

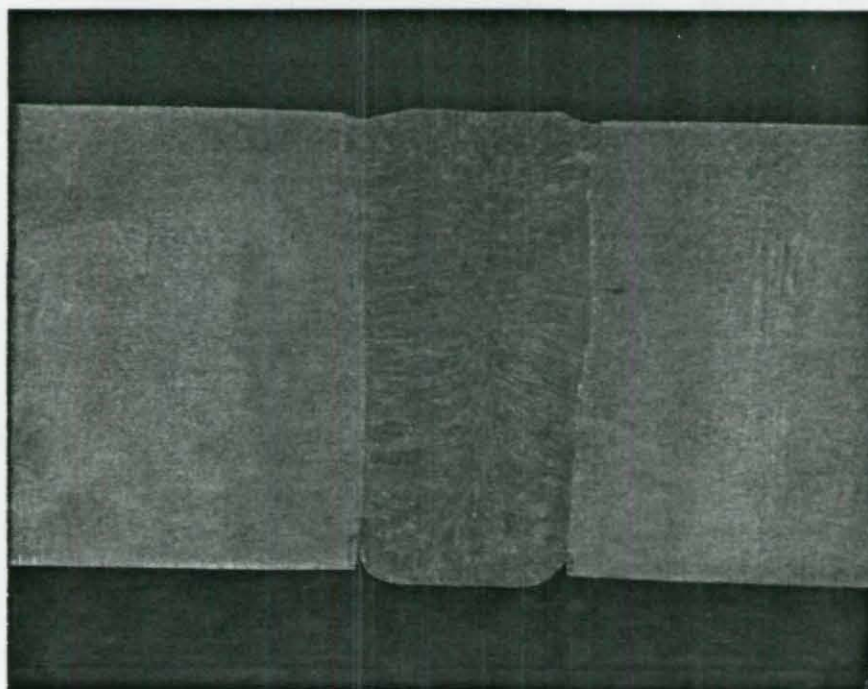


Figure 10. Metallographic Section, Welded Test Plate No. 5A. Note Lack of Fusion Defect (Slag Entrapment) at Root of Weld. Magnification 1.2 x.

Table 7

HEAT AFFECTED ZONE WIDTH AT MIDTHICKNESS OF PLATE
A 588 Grade H Plate

<u>I.D. No.</u>	<u>Heat Affected Zone Width (in.)</u>
3A	0.459
5A	0.574
7A	0.426
9A	0.500
13A	0.451
15A	0.566
17A	0.401
21A	0.459

on both sides of the root for test weld 5A shown in Figure 10. Comparing Figures 9 and 10, one notes a slightly larger weld metal grain size and larger heat affected zone width for weld 5A relative to weld 3A consistent with the higher heat input used. Heat affected zone width measurements in Table 7 also reflect the higher heat input. Figures 11 and 12 show the weldment microstructures observed for test plates 7A and 9A. Comparison of Figures 11 and 12 shows little difference between these welds in terms of weld metal grain size. Heat affected zone width is slightly different for the two welds as shown in Table 7 but this difference is inversely correlated with welding process heat input.

Figure 13 shows the weldment microstructure observed for test plate 13A. The weld metal shows a much larger columnar grain size than for the higher alloy content welds shown in Figures 9-12. The heat affected zone width shown in Table 7 for weld 13A is not as small as might be expected for the low heat input used to prepare this weld. Figure 14 shows the weldment microstructure observed for test plate 15A prepared with the Linde 95 high alloy electrode and no powder additions. Compared to the analogous powder addition welds 7A and 9A shown in Figures 11 and 12, this weld shows a much larger weld metal grain size consistent with the higher heat input used to prepare it. The heat affected zone width shown in Table 7 is among the larger values measured, again consistent with high process heat input.

Detailed metallographic examination was performed on cross sections of welds 9A, 13A, and 15A. Figure 15 a-c shows the microstructure observed for weld 9A. In Figure 15a, the weld metal microstructure at the quarter width location, i.e. in the center of the columnar grained region, is shown. Figure 15b shows the microstructure observed at the weld fusion line while Figure 15c shows the microstructure of the heat affected zone immediately adjacent to the fusion line where the most extreme grain coarsening occurs. For comparison, Figure 16 a-c shows the microstructures observed for the same locations in weld 15a which was produced using the same Linde 95 filler metal but with no metal powder additions. Comparing Figures 15a and 16a shows that the grain size in the columnar grained region of the powder addition weld (9A) is reduced by approximately

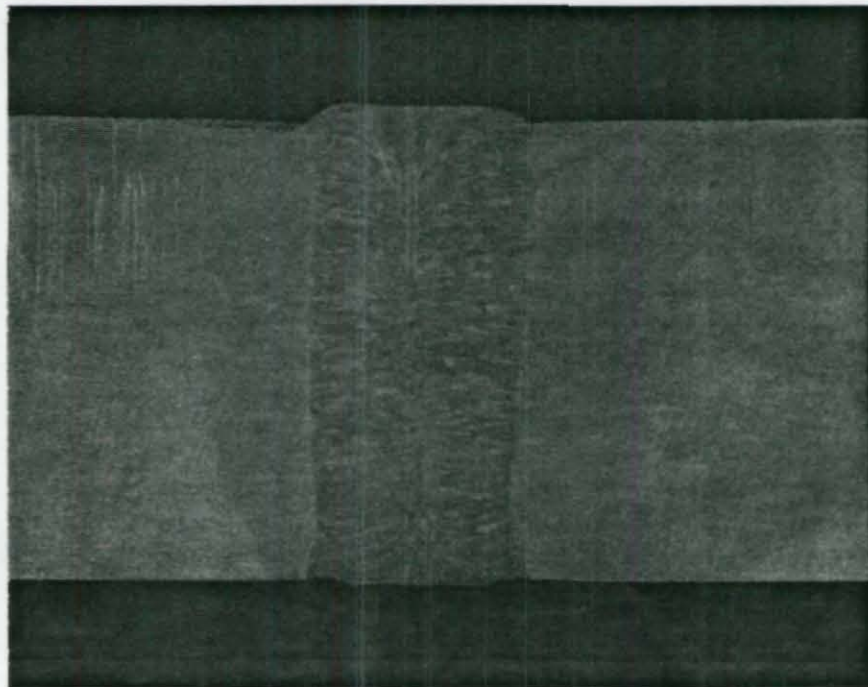


Figure 11. Metallographic Section, Welded Test Plate No. 7A. Magnification 1.2 x.

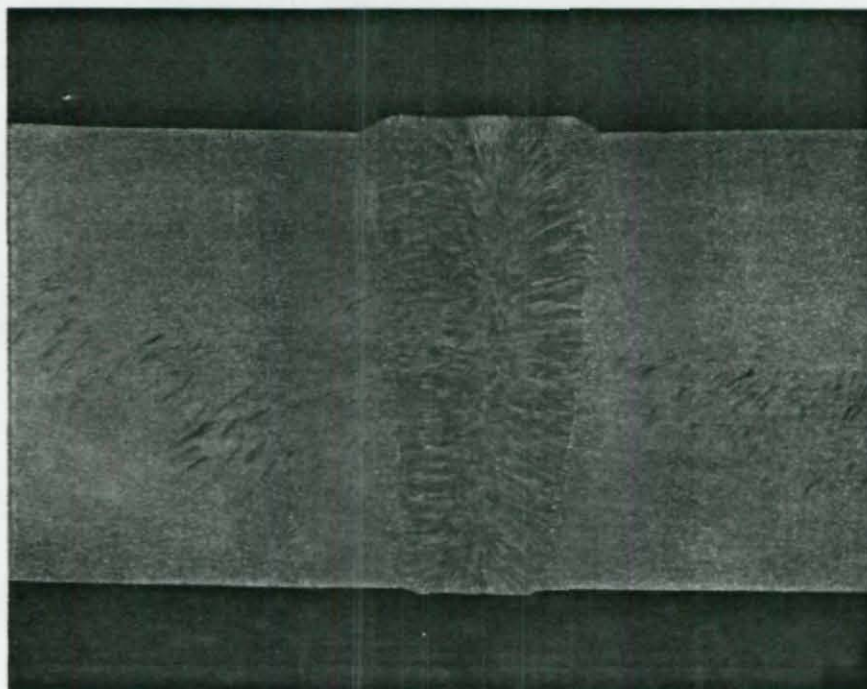


Figure 12. Metallographic Section, Welded Test Plate No. 9A. Magnification 1.2 x.

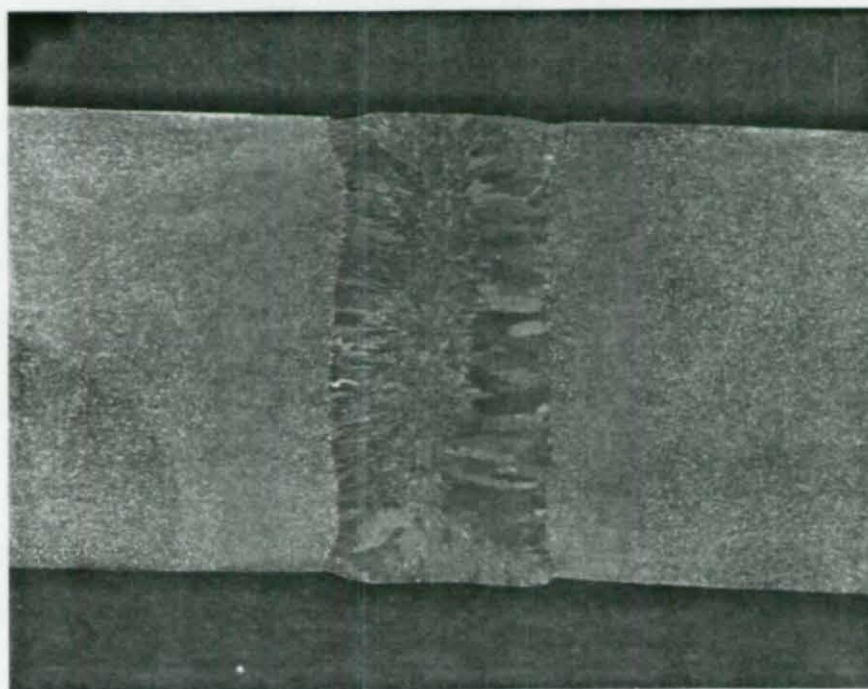


Figure 13. Metallographic Section, Welded Test Plate No. 13A. Magnification 1.2 x.

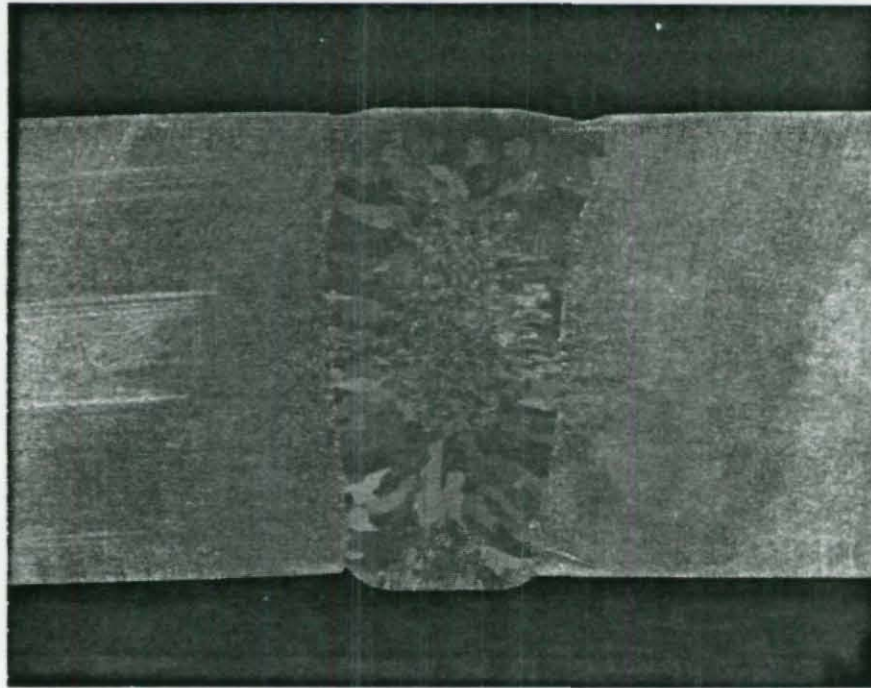


Figure 14. Metallographic Section, Welded Test Plate No. 15A. Magnification 1.2 x.

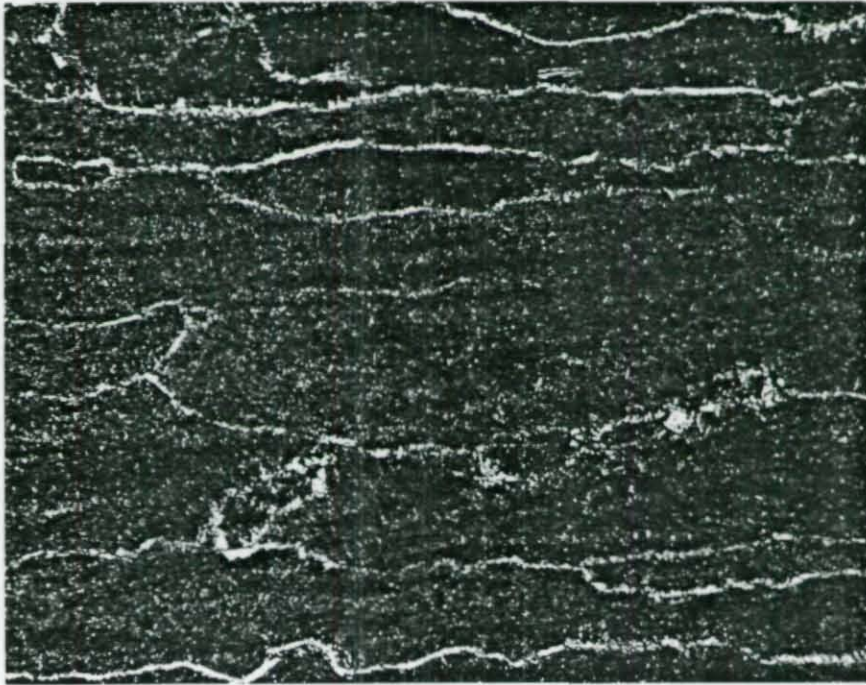


Figure 15a. Weld Metal Columnar Grained Microstructure 9A. Magnification 1.2 x.

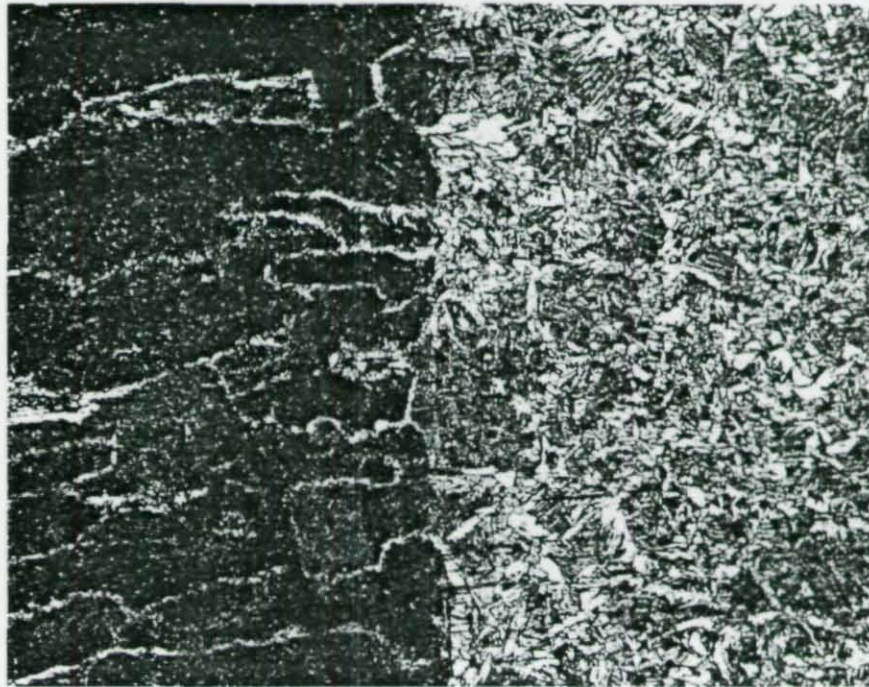


Figure 15b. Fusion Line Microstructure, Weld Metal to Left, Weld 9A.
Magnification 50 x.

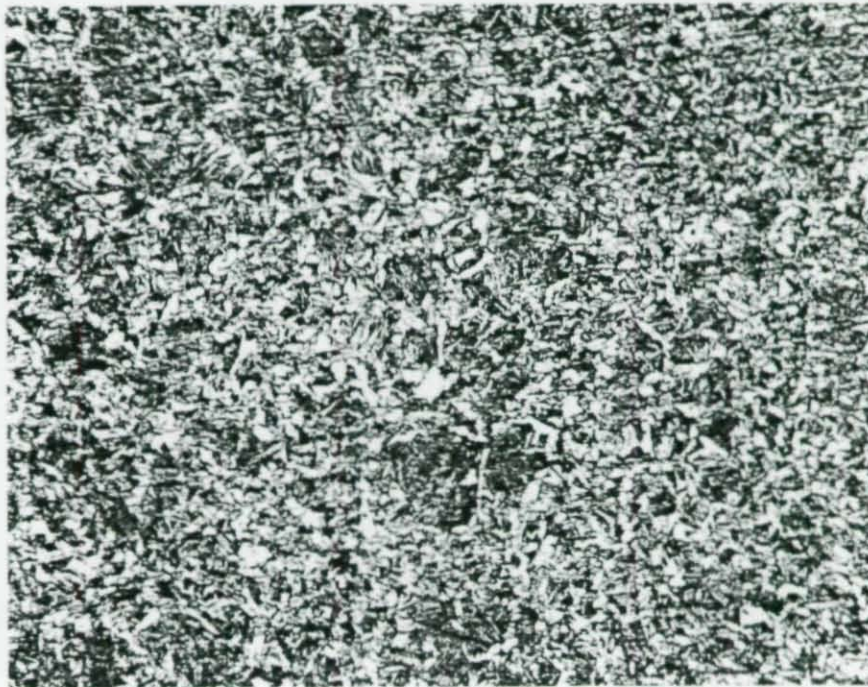


Figure 15c. Heat Affected Zone Microstructure Adjacent to Fusion Line,
Weld 9A. Magnification 50 x.



Figure 16a. Weld Metal Columnar Grained Microstructure, Weld 15A. Magnification 50 x.

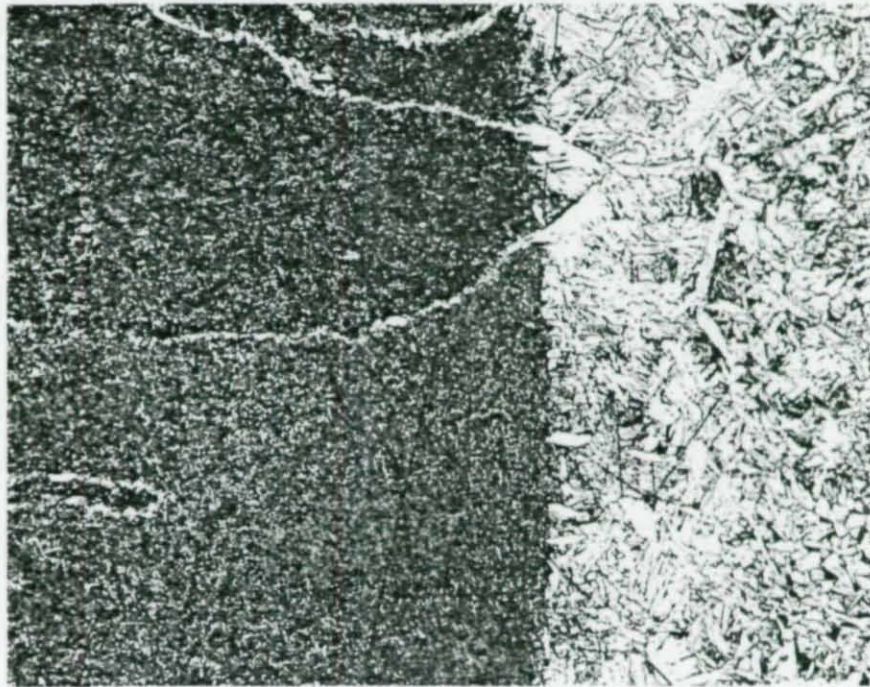


Figure 16b. Fusion Line Microstructure, Weld Metal to Left, Weld 15A.
Magnification 50 x.

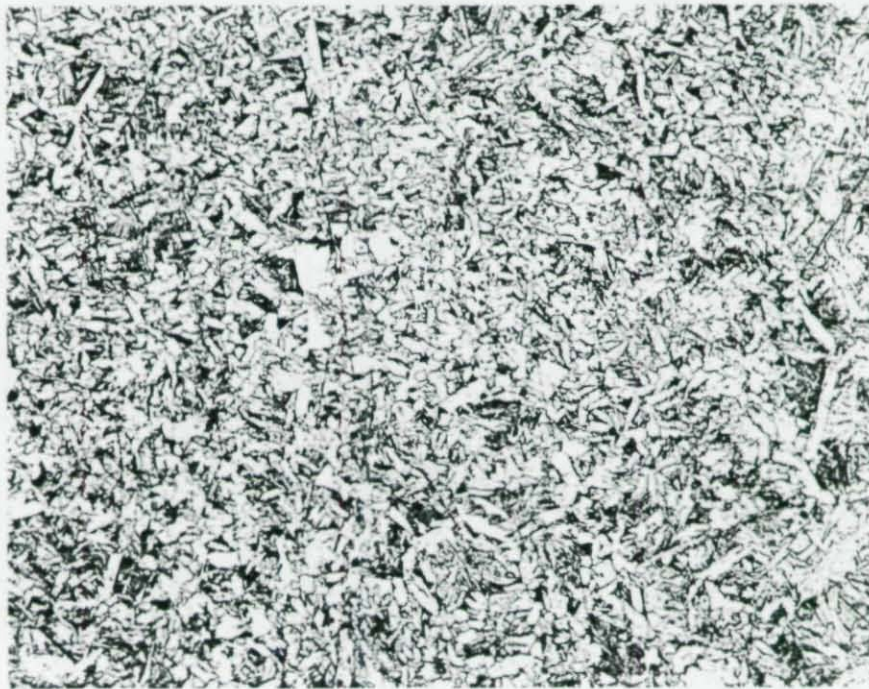


Figure 16c. Heat Affected Zone Microstructure Adjacent to Fusion Line,
Weld 15A. Magnification 50 x.

a factor of two relative to the weld produced without powder addition (15A). Comparing Figures 15b and 16b show a similar reduction in weld metal grain size for the powder addition weld adjacent to the fusion line. These figures also show a slightly reduced grain size in the heat affected zone of the powder addition weld adjacent to the fusion line compared to the weld produced with no powder additions. Figures 15c and 16c similarly show reduced grain size in the heat affected zone of the powder addition weld.

Figures 17 a-c show the microstructures observed for the lower alloy content powder addition weld 13A. Comparing the high alloy powder addition weld (9A) shown in Figures 15 a-c to weld 13A in Figures 17 a-c shows a much larger weld metal columnar zone grain size in the low alloy weld 13A, even though the low alloy weld was produced at a significantly lower heat input. Comparing Figures 15b and 17b shows a similarly larger weld metal grain size adjacent to the fusion line of the low alloy content weld. Thus it appears that weld metal grain size is significantly affected by alloy content in the powder addition welds. The large grain size at the fusion line and the low weld metal alloy content may account for the low fusion line impact strength described above for weld 13A. Comparing Figures 15c and 17c shows that the heat affected zone microstructures for these two powder addition welds are virtually identical.

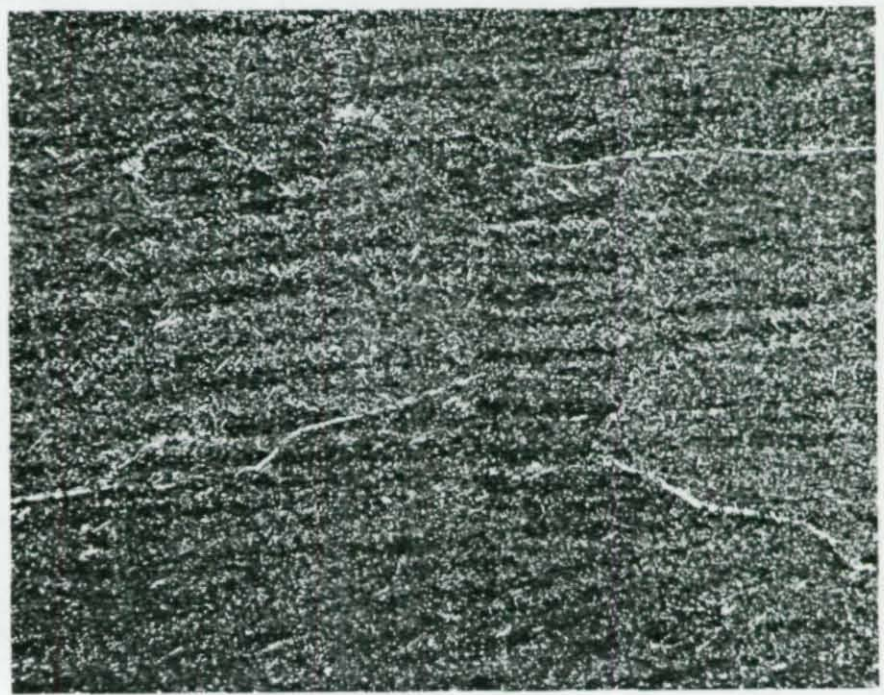


Figure 17a. Weld Metal Columnar Grained Microstructure, Weld 13A. Magnification 50 x.

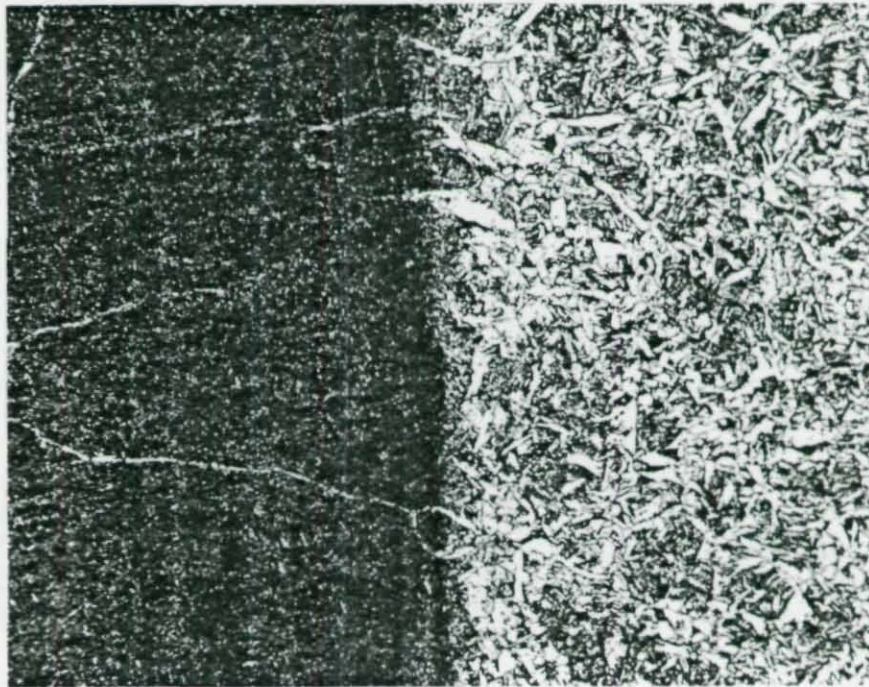


Figure 17b. Fusion Line Microstructure, Weld Metal to Left, Weld 13A.
Magnification 50 x.

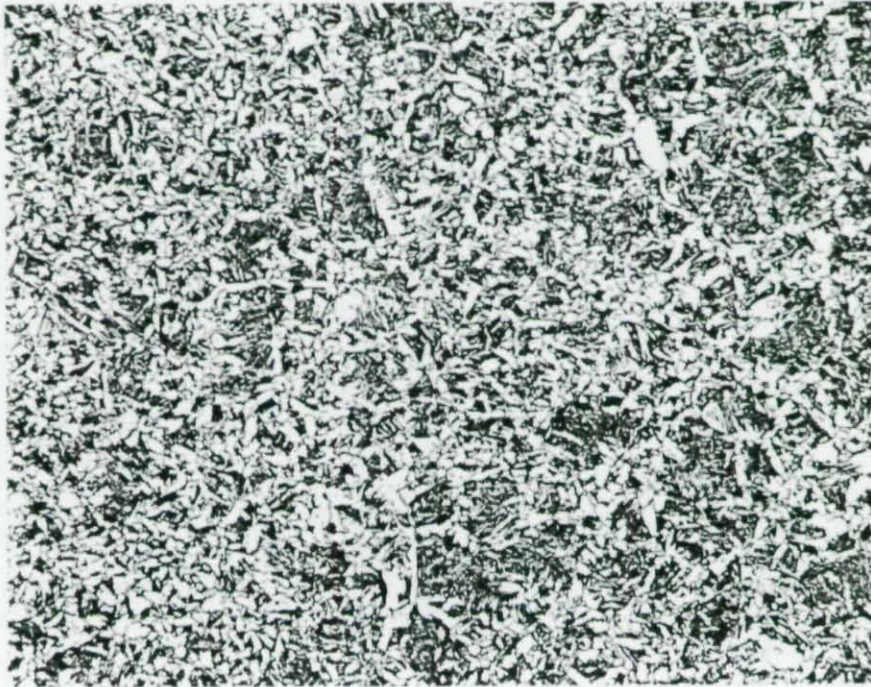


Figure 17c. Heat Affected Zone Microstructure Adjacent to Fusion Line,
Weld 13A. Magnification 50 x.

Flux-Cored Electrodes

Two experimental welds were prepared using 0.062 in. diameter flux-cored, high alloy electrodes. Both were prepared with metal powder/electrode weight ratios of 0.6.

Table 2 shows the welding process parameters used to prepare each of the experimental welds. Weld 17A was prepared using the Hobart Fabco 805 electrode/FC-727 powder combination. Weld 21A was prepared using the Linde FC-727 electrode/FC-727 powder combination. Filler metal compositions were shown in Table 1. It should be noted that the deposition rates are significantly lower for the flux-cored electrode/powder combinations than for the solid electrode/powder combinations previously described. At the same time, welding process heat input is higher for the flux-cored electrode/powder combinations due to the significantly lower vertical travel speed used. Linde 124 flux was used as a starting flux to establish the electroslog mode. Since the wire core contains a significant amount of flux, no additional flux was added during welding.

Table 3 shows the results of chemical analyses of the weld metal of each of the two welds at the center/center location. Welds 17A and 21A show almost identical compositions which, compared to the solid electrode welds, are lower in Mn and higher in Ni. The analyses are consistent with the electrode and powder compositions shown in Table 2 and with the powder/electrode weight ratios used.

The results of longitudinal and transverse tensile tests on these two welds are shown in Table 4. Yield and tensile strengths are similar to those observed for the solid electrode welds. Elongation and reduction in area are lower for the flux-cored electrode welds, however. Weld 17A shows the anisotropy of tensile properties observed for most of the solid electrode welds while weld 21A does not.

Screening Charpy V-notch impact test results for welds 17A and 21A for the weld metal centerline and heat affected zone (fusion line plus 2.0mm location) are shown in Table 5. Weld metal impact strength for both flux-cored electrode welds are significantly lower than for the solid electrode/powder addition welds. Heat affected zone impact strength

values are similar to the lowest values observed for the solid electrode welds and are consistent with the high heat inputs used to prepare welds 17A and 21A. It thus appears that the flux-cored, high alloy electrodes are unlikely to provide the same level of weldment impact properties which can be obtained with the best of the solid electrode/powder combinations, although the level of properties provided is still significantly higher than for conventional electroslag welds and significantly better than for the low-alloy flux-cored electrode welds produced in the original AISI-sponsored research.

Metallographic sections of welds 17A and 21A are shown in Figures ¹⁸~~15~~ and ¹⁹~~16~~, respectively. These sections reveal a major problem with the flux-cored electrodes. An excessive amount of flux is contained in the wire core leading to incomplete filling of the joint with weld metal. This could be corrected to a limited extent by changing the reinforcement design in the water-cooled copper shoes but would be best corrected by reducing the amount of flux contained in the wire core. Both flux-cored electrode/powder addition welds show finer weld metal grain size than the solid electrode/powder addition welds shown in Figures 9-13. Heat affected zone widths for these two welds, shown in Table 7, are somewhat less than might be expected on the basis of calculated welding process heat input.

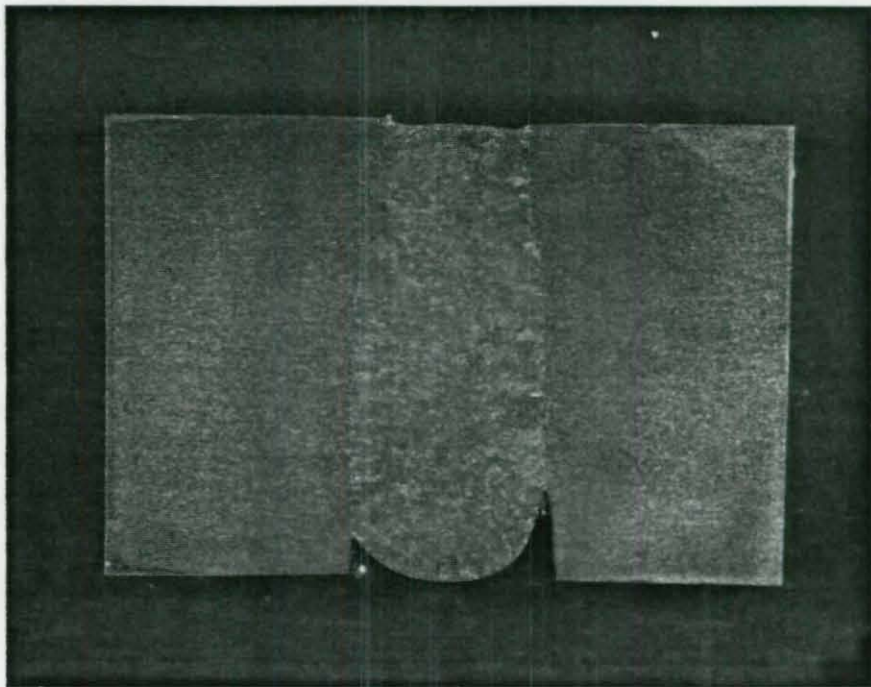


Figure 18. Metallographic Section, Welded Test Plate No. 17A. Magnification 1.2 x. Note Incomplete Joint Fill Caused by Excessive Flux Content.

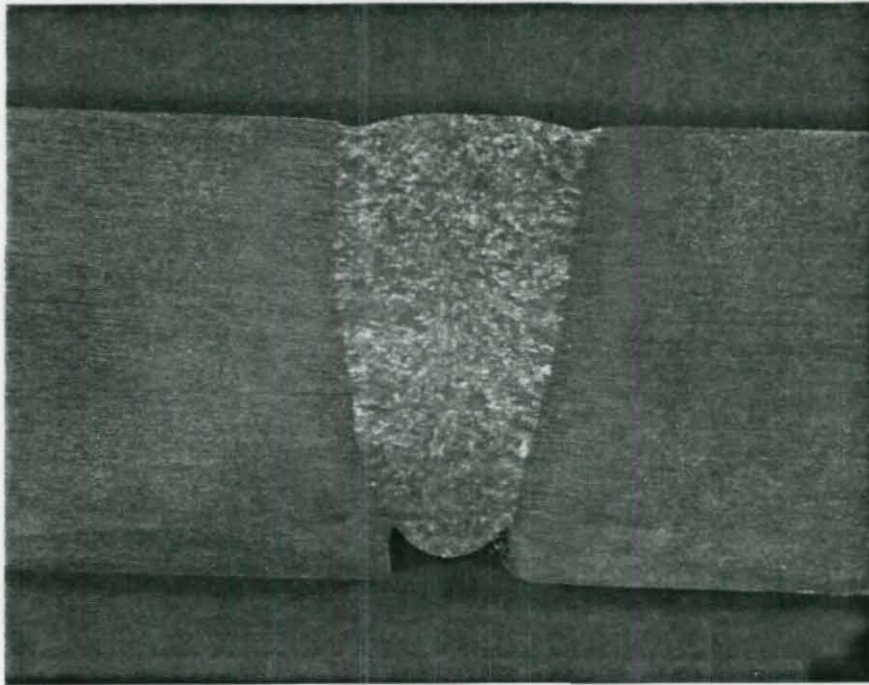


Figure 19. Metallographic Section, Welded Test Plate No. 21A. Magnification 1.2 x. Note Incomplete Joint Fill Caused by Excessive Flux Content.

CONCLUSIONS

The high alloy content solid electrode, metal powder addition electroslag welds show significantly higher weld metal and heat affected zone impact strengths than do conventional electroslag welds in A588 steel. This is due to a combination of reduced welding process heat input for the metal powder addition welds which results in finer weld metal and heat affected zone grain sizes and to the higher alloy (particularly Ni) content of the weld metal. Lower alloy (particularly Ni) content powder addition electroslag welds showed inferior weld metal and heat affected zone impact strengths to the high alloy welds but these impact strengths still far exceeded those usually observed for conventional electroslag welds. Tensile properties of the high alloy and low alloy welds were similar and easily exceeded the requirements for A588 welds.

Flux-cored electrode, high alloy content powder addition electroslag welds showed inferior impact properties but similar tensile properties to the solid electrode welds. Impact properties of these flux-cored welds were also superior to those usually observed for conventional electroslag welds in A588. The high alloy flux-cored electrodes contained excessive amounts of flux in the electrode core which consistently led to incomplete joint fill during welding and retained slag in the weld joint. Reduction of flux content in the electrode core would thus be desirable to facilitate use of these electrodes in electroslag welding.

The metal powder addition electroslag welding process using high alloy content filler metals appears to provide greatly improved weldment properties relative to conventional electroslag welds in A588 steel. This is expected to provide improved reliability of electroslag welded structures when the process is implemented by structural steel fabricators. Reduced fabrication costs are also expected from implementation of the powder addition electroslag welding process because of increased filler metal deposition rates and reduced filler metal costs.

RECOMMENDATIONS

The very encouraging results obtained in this project on reduced heat input electroslag welding of A588 steel using high alloy electrodes and metal powder additions have been obtained with a travelling-head type welding apparatus. This type of equipment is commonly used in the shipbuilding and pressure vessel fabrication industries. Structural steel fabrication, however, is more commonly performed using consumable guide tube electroslag welding equipment. Reduced heat input electroslag welding has never been demonstrated using the consumable guide tube process. Additional research should be performed to develop a metal powder addition, reduced heat input, consumable guide tube electroslag welding process and produce experimental welds using high alloy content electrodes and powders. These welds should be evaluated in detail for comparison to the travelling-head welds already produced. The project would have as its objective the demonstration of a simplified electroslag process for use by structural steel fabricators capable of providing both greatly improved weldment properties and welding process productivity.

Research performed in this project has shown very significant improvements in CVN toughness of reduced heat input, high alloy electroslag weldments in ASTM A588 steel. Weld metal and heat affected zone minimum impact strengths have been improved by as much as an order of magnitude compared to conventional electroslag welds. Additional information is required on improvements in fatigue strength and fracture toughness of the improved weldments relative to their conventional counterparts. Research should therefore be undertaken to measure fatigue resistance, for both baseline and reduced heat input high alloy welds, of weld metal and composite (weld plus heat affected zone) specimens in both reversed bending and tension-tension modes. Plane strain fracture toughness should be measured for weld metal, heat affected zone, and base metal locations. Fatigue and fracture toughness data should be obtained as a function of welding process heat input and correlated with weldment composition and microstructure. Engineering data developed in such additional research would be extremely important in determining the ultimate utility of the improved process in structural steel fabrication.

01683